Decolourisation of methylene blue and congo red dye solutions by adsorption using chitosan

Abdallah Rahali[a,b], Ali Riazi[b], Badredine Moussaoui[b], Ahmed Boucherdoud[c,]*, Nihal Bektaş[d]

[a]*Agronomy department, Institute of Exact Sciences and Sciences of Nature and Life Ahmed Zabana University Center, Relizane – Algeria, email: Rahali28@live.fr (A. Rahali)*
[b]*Laboratory of Beneficial Microorganisms, Functional Foods and Health, University of Mostaganem – Algeria, emails: Ardz22003@yafoo.fr (A. Riazi), moussmed@hotmail.fr (B. Moussaoui)*
[c]*Chemistry department, Institute of Exact Sciences and Sciences of Nature and Life Ahmed Zabana University Center, Relizane – Algeria, email: bo-ahmed@live.fr (A. Boucherdoud)*
[d]*Environmental Engineering Department, Gebze Technical University, 41400 Gebze, Turkey, email: bektasn@gmail.com (N. Bektaş)*

ABSTRACT

Water pollution from industrial discharges is a worldwide problem and can have very harmful effects on the environment. In this study, adsorptive removal of two different dyes was investigated using a new natural, biodegradable adsorbent based on shrimp shells: chitosan in a batch adsorption operating system. Chitosan was synthesized from flowery prawn and then characterized using different analytical techniques. The results obtained show a remarkable removal rate in the first 30 min with optimum process conditions for both dyes. Linear forms of pseudo-first-order, pseudo-second-order kinetic, and the intra-particle diffusion kinetic model equations were used to describe the kinetic data of the dye removal process. The Langmuir and Freundlich adsorption isotherm models were used to analyze equilibrium data of adsorption of dyes by chitosan. The maximum adsorption capacities (Q_m) of chitosan for methylene blue and congo red dye were in the range of 116.3 and 113.6 mg g^{-1}, respectively. The study shows that the dye adsorption process on chitosan can be described as both isotherm models used.

Keywords: Adsorption; Methylene blue; Congo red; Chitosan

1. Introduction

Industrialization, unplanned urbanization, agricultural activities due to the rapid growth of the world's population caused the excessive use of chemicals resulting in the discharge of chemical pollutants into the environment [1,2]. Non-natural dyes can be used in a great amount as a colorant in various industries such as paper, leather, paint along with textile industries. The necessity of high rate water usage in dying processes, a great amount of colorant wastewater is generated in these types of industries. In general, the wastewater discharged in a textile operation is approximately in the range 40–65 L kg^{-1} of the product. A wide range of different classes of dyes disperse, including reactive, basic, acid, direct, azoic, and sulfur dyes can be used in the textile industry [3,4]. Insoluble dyes are can be separated from the wastewater by various methods while other water-soluble dyes can be hard to treat by the conventional separation process.

* Corresponding author.

The release of colored substances into receiving media may lead to aesthetic problems, reduce light penetration, inhibit photosynthesis, and highly be harmful to humans, living other *organisms and environments* [3,7]. Therefore, strict discharge limits and guidelines for effluent containing dyes are being set by Governments and Environmental Agencies in many countries, resulting in the necessity of advanced treatment of colored wastewater. There are many different physical and chemical treatment methods that are available for treating textile wastewater [8–11]. Besides these methods, adsorption is the simplest and the easiest method and still the preferred method for an effective and economical way to treat wastewater, especially recycled waste materials used as adsorbents in the treatment. Several research papers reported for a dye removal process using natural adsorbents [12–14].

Chitosan has been widely used in the production of different biological medical products [15]. Chitosan is made from crustacean exoskeleton chitin, the cuticles of insects by deacetylation of acetoamide groups at high pH value. After cellulose, chitosan is known as the most widely found biopolymer in the world. Great amounts of amino groups in chitosan provide very suitable properties for adsorption of heavy metals such as Cu^{2+}, Cd^{2+} and Pb^{2+} with an adsorption capacity of 0.27, 0.036 and 0.016 mmol g^{-1}, respectively [16–19] and organic dyes like acid green 25 and reactive blue 222 with 645.1 and 87.3 mg g^{-1} adsorption capacity [20,21]. The polycationic feature of the polymer is created by protonating the deacetylated amino groups in chitosan and these groups are served to provide charged connections with pollutants.

In this study, chitosan, a low-cost natural adsorbent, was used for the adsorptive removal of methylene blue (MB) and congo red (CR). The characteristics of chitosan were determined using different analytical methods and different parameters affecting the adsorption processes such as pH, adsorbent mass, and dye concentration were investigated. Then equilibrium and kinetic results of dye removal were investigated and compared to different models.

2. Materials and methods

2.1. Materials

MB and CR from (Merck, Germany), ethanol from Chem Lab (South Africa), sodium hydroxide (NaOH) and hydrochloric acid (HCl) from Sigma-Aldrich (USA). All chemicals used in the experiments were very high grade and used without any extra treatment. Distilled water was used through the experiments.

2.2. Preparation of adsorbents

Flowery prawn heads were obtained from a prawn processing facility and adsorbent preparation steps are given in Fig. 1. The prawn shells were first separated from their heads to remove unwanted wastes and washed thoroughly to remove meat residue and additional impurities. The shells were dried in an oven at 105°C until a fixed weight was achieved. After this heating process, prawn shells were ground and separated to obtain particles of size smaller than 250 μm [22,23].

The shrimp powder obtained is passed through the demineralization step. Shells were cured with 0.25 M HCl solution in the room temperature with a ratio of 1:40 w/v (1 g of shell per 40 mL of HCl), solid and minerals inside the prawn shell are dissolved into acid during this demineralization process [22,23]. The demineralization
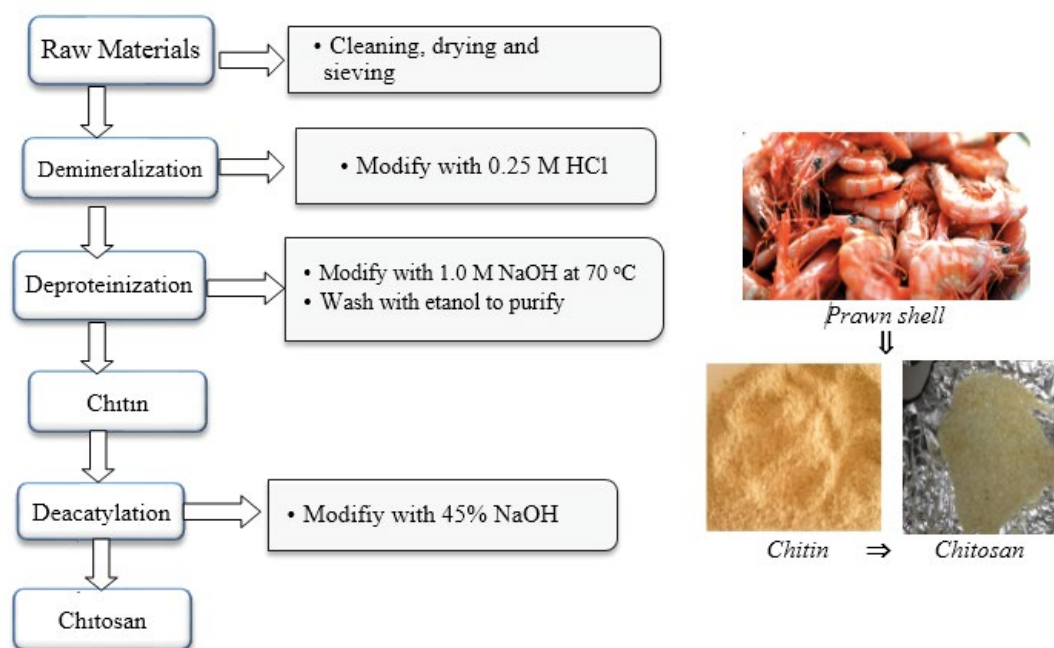
Fig. 1. Preparation of chitosan from flowery prawn.

Table 1
Chemical structure and characteristics of adsorbed dye

	Methylene blue	Congo red
Structure		
CI	52015	22120
Molecular formula	$C_{16}H_{18}ClN_3S \cdot 3H_2O$	$C_{32}H_{22}N_6Na_2O_6S_2$
Molecular weight (g mol^{-1})	319.8	696.6
Maximum wavelength λ_{max} (nm)	660	495
Supplier	Merck	Merck
Water solubility (g L^{-1})	44	25
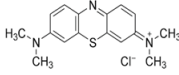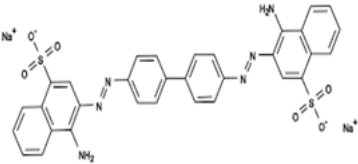
process helps to minimize the ash content and the carbonates and phosphates which present in the solid. Distilled water was used to clean this created solid for removing dissolved minerals and excess HCl. Afterward, the solid sample was put into an oven at 105°C until a fixed weight was reached.

Demineralized prawn shell powder was achieved by treating the prawn powder from previous steps with 1.0 M NaOH by heating to 70°C with a solution to a solid ratio of 20 mL g^{-1}. In this process, the proteins in the solid are dissolved in NaOH due to the conversion of the protein into the water-soluble amino acids. The modification was repeated numerous times until no color seen meaning settling of medium solids indicates the on-existence of protein. The resultant solid was then washed to get neutral to eliminate suspended protein and excess NaOH [20,21]. Then the samples were dried in the oven at 105°C to a constant weight. After this step, the resulting powder was first washed with hot ethanol (solution to solid ratio of 10 mL g^{-1}) and later boiled in acetone (solution to solid ratio of 10 mL g^{-1}) to eliminate other small amounts of impurities can be present in the prawn shells [18] as a purification step. Distilled water was used to clean purified powder (chitin) and then dried in an oven at 105°C to a fixed weight.

The last step is the preparation of chitosan known as deacetylation. In this step, chitin is converted to chitosan by the removal of acetyl groups known as the deacetylation process. Chitin was immersed in a 45% NaOH solution (solution to solid ratio of 15 mL g^{-1}) at 22°C for 4 days and then washed with distilled water until a pH value of 7 and dried in the oven at 105°C to a constant weight [18]. Deacetylation degree of chitosan was valued using the Fourier-transform infrared spectroscopy (FTIR) in the range of 500–4,000 cm^{-1}.

2.3. Samples characterizations

The chitosan used along this experiment is characterized by FTIR of the (Shimadzu IR Prestige-21, Japan) with potassium bromide (KBr) tablets as a reference at the frequency range 400–4,000 cm^{-1}.
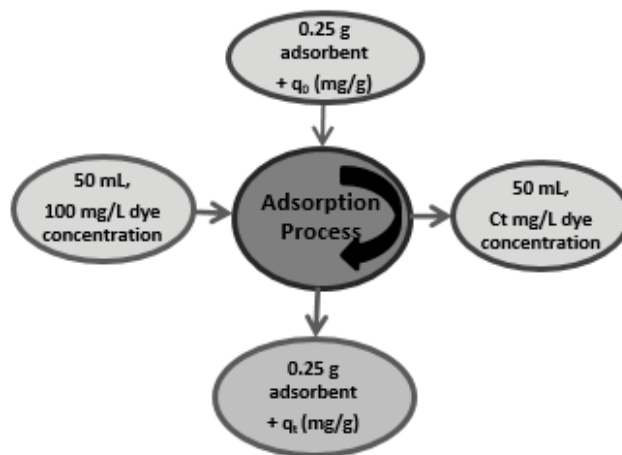
Fig. 2. Schematic for batch adsorption experimental set-up used.

Zeta potential of the biopolymer used in the experiments was measured by Zetasizer 2000 system (Malvern Instruments Ltd., Worcestershire, UK) to see changes in the charge of chitosan according to different pH values 3–9.

Degrees of acetylation (DA) and deacetylation (DDA) are essential parameters for characterizing chitosan. The degree of acetylation (DA) relates to the N-acetylamine groups [24]. The degree of deacetylation (DDA) shows the removal of the acetyl group from the chain and can be determined by FTIR analysis from Eqs. (1) and (2). The degree of deacetylation of chitosan was calculated using the common equation given as follows [25]. The absorbance values at 1,650 and 3,450 cm^{-1} are the absolute heights of absorption bands of amide and hydroxyl groups respectively [26].

$$DA = \frac{A_{1,650\,cm^{-1}}}{A_{3,450\,cm^{-1}}} \frac{100}{1.33} \tag{1}$$

$$DDA\% = 100 - DA \tag{2}$$

The surface of chitosan is also characterized by a scanning electron microscopy coupled with energy-dispersive X-ray spectroscopy (SEM-EDS) (Philips XL 30 SFEG, Germany).

2.4. Adsorption experiments

The adsorption experiments were investigated in batch operation type at different initial values of pH, temperature, and dye concentration (Fig. 2). The adsorption experiments were performed by introducing a precisely weighed amount of chitosan (0.25 g) into a volume of 50 mL of 100 mg L^{-1} synthetically prepared two different dye solutions. The experiments were conducted with adding chitosan to 50 mL of the MB solution at a constant temperature of 25°C.

Two series of isotherm plots were achieved for two different dye solutions and each isotherm studies contained five dye concentrations ranged from 10 to 150 mg L^{-1}. For each experiment cycle, separate flasks were prepared and used to evaluate the experimental data. At each time, the adsorbent was removed from solution by centrifugation at 2,600 rpm for 4 min and final dye concentrations were measured in the solutions using a UV-Vis spectrophotometer (Hach Lange, DR 2800, Germany) spectrophotometer at the wavelength corresponding to the sample's maximum absorbance value.

The adsorption capacities of each dye were calculated using Eq. (3) and other parameters were measured experimentally.

$$q_t = \frac{V(C_0 - C_t)}{m} \tag{3}$$

where q_t (mg g^{-1}) is the amount of dye adsorption per unit of adsorbent at the time, C_0 and C_t (mg L^{-1}) are the initial concentration and the concentration at the time, respectively; m is the mass of adsorbent used (g) and V is the volume of solution (L).

Adsorption kinetics define the reaction pathways the rates and process mechanism until the equilibrium. Different kinetic models are used:

Pseudo-first-order: described the kinetics of adsorption of a species in an adsorbent by the ordinary first-order differential equation which gives by integration the following equation [27,28]:

$$\log(q_e - q_t) = \log(q_e) - \frac{k_1}{2.303}t \tag{4}$$

where q_t and q_e (mg g^{-1}) is the amount of dye adsorption per unit of adsorbent at time t (min), and at equilibrium respectively, k_1 is the pseudo-first-order rate constant (min^{-1}) calculated from the plot of $\log(q_e - q_t)$ against t.

Pseudo-second-order: In this model, the binding of pollutants to the surface of the adsorbent is due to the physicochemical interactions between the adsorbent and the adsorbate, which leads to a chemisorption process [29]. The linear form of this model given by Eq. (5) [30].

$$\frac{t}{q_t} = \frac{1}{k_2' q_e^2} + \frac{1}{q_e}t \tag{5}$$

where k_2' (g mg^{-1} min^{-1}) is the rate constant for the pseudo-second-order model, used to calculate the initial adsorption rate (h) (mg g^{-1} min^{-1}) [Eq. (6)]. The values of h, k_2', and q_e calculated from the plot of t/q_t against t.

$$h = k_2' q_e^2 \tag{6}$$

Intra-particle diffusion model has been used to interpret the adsorption process of MB and CR by chitosan, this model can be represented by Eq. (7) [31].

$$q_t = k_i t^{(1/2)} \tag{7}$$

where k_i is the intra-particle rate constant (mg g^{-1} min$^{1/2}$).

Adsorption isotherm expresses the difference of concentration of solute at liquid and solid phases at equilibrium. In this study, the adsorption process was investigated by Langmuir and Freundlich isotherm models. In Langmuir model [Eq. (8)], only homogenous adsorption takes place on the solid surface and a place can only have occupied by one solute and no more adsorption can occur at this surface [32].

$$\frac{C_e}{q_e} = \left(\frac{1}{Q_m b}\right) + \left(\frac{1}{Q_m b}\right)C_e \tag{8}$$

where C_e (mg L^{-1}) is the concentration of dyes at equilibrium, Q_m is the maximum adsorption capacity (mg g^{-1}) and b (L mg^{-1}) is the constants of Langmuir isotherm.

A dimensionless separation parameter (R_L), can also be calculated from Langmuir equation [33]. R_L values calculated shows the description of adsorption type Eq. (9), for example, either unfavorable ($R_L > 1$), linear ($R_L = 1$), favorable ($0 < R_L < 1$), or irreversible ($R_L = 0$) [34,35].

$$R_L = \frac{1}{1 + bC_0} \tag{9}$$

The empirical Freundlich isotherm Eq. (10) can be used to describe non-perfect and multi-layer adsorption on heterogeneous surfaces [36]. The constant n linked to the adsorption intensity while K_F connected to the adsorption capacity (mg g^{-1}) [37].

$$\log q_e = \log K_F + n \log C_e \tag{10}$$

K_F (mg g^{-1}) (L mg^{-1})$^{1/n}$, and n are Freundlich isotherm model constants which relate to the capacity and the intensity of adsorption respectively [37,38]. The ratio $(1/n)$ is a function of the adsorption force and measures the surface heterogeneity [39,40]. If $n = 1$ then the partition between the liquid and solid phase is independent of the concentration while the adsorption is linear [41], If the value of $(1/n) > 1$, this indicates cooperative adsorption, However, $(1/n) < 1$ than one indicates normal adsorption [42].

3. Results and discussion

3.1. Characteristics of chitosan

3.1.1. Infrared characterization of chitosan

FTIR spectroscopy of chitosan Fig. 3 shows that the elongation vibration located at 3,429 cm^{-1} marks the occurrence of amine group N–H. In fact, the bands corresponding to the symmetrical valence vibration of the CH$_3$ group and that of the C–H elongation were respectively 2,924 and 2,893 cm^{-1}. There was also a C–C vibration from the aromatic ring at 1,577 cm^{-1} and an N=N vibration at 1,485 cm^{-1}. In addition, the C–N elongation vibration appeared at 1,379 and 1,179 cm^{-1}. There was also a band at 1,103 cm^{-1} which corresponds to S=O vibration. The vibration of deformation in the plane of C–H is at 1,026, 811.59 and 689.34 cm^{-1}. Finally, a band at a C–S vibration appeared at 582.13 and 536.05 cm^{-1}. However, After the adsorption of MB and CR on chitosan, we observe the appearance of two peaks around 900 and 554 cm^{-1} corresponds to C=C aromatic of dyes [4], on the other hand; a decrease in the intensity of the peaks 1,379 and 1,577 cm^{-1} which corresponds to (C–N), and aromatic ring respectively due to the electrostatic interaction between these groups and the sulfur atom from MB and a sulfonated group of CR [43], another obvious change is observed at the frequency level 3,429 cm^{-1}, which indicates the participation of amino groups in the adsorption process [44]. These changes after adsorption of dyes proved that a chemical contact happened between the chitosan and dye molecules, as the main functional groups engaged in the adsorption process of both dye molecules on chitosan were the amine groups [45,46].

3.1.2. Zeta potential of chitosan

pH$_{pzc}$ (pH at which the electrical charge is zero on the surface of the adsorbent) is a very important parameter explaining the adsorption process in terms of electrostatic attractions between the charged surface of the adsorbent and the pollutants, the pH$_{pzc}$ of chitosan is measured in a pH range between 3 and 9 corresponding to potential values between 10.6 mV and –9.88 mV, the zeta potential result of chitosan at different pH values is shown in Fig. 4. The pH$_{pzc}$ of chitosan decreases almost linearly with increasing the pH, the optimal value of pH$_{pzc}$ obtained is 6.5. It is significant to indicate that at pH > 6.5 the chitosan's negatively surface charged. On the other hand; at pH < 6.5 the surface of chitosan is a positive charge. The positive charge of chitosan is achieved by protonation of the amine group in NH$_3^+$ form after its solubilization in acetic acid. This can be referred to the protonation mechanism of chitosan [47]. In an acidic environment, chitosan (Chit-NH$_2$) can act as a weak base and reacts with the H$^+$ protons resulting from the acetic acid dissociation to produce the chitosan with protonated form (Chit-NH$_3^+$) according to the following stable reaction Eq. (11):
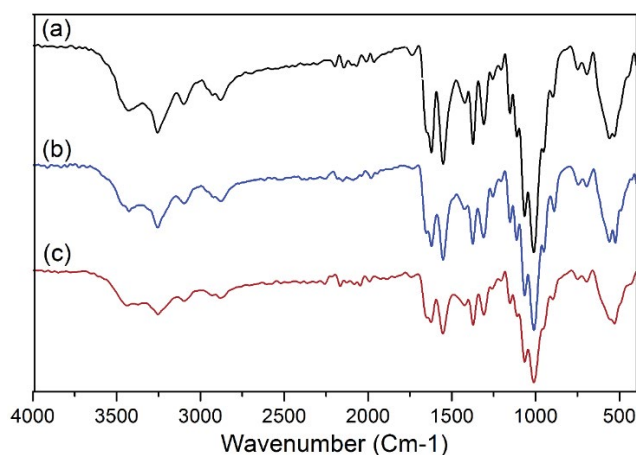
$$Chit - NH_2 + H^+ \rightarrow Chit - NH_3^+ \tag{11}$$
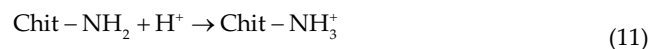
When the pH has been increased, there is a reduction in the zeta potential of chitosan due to the neutralization of chitosan by an excess NaOH. Strong hydroxyl groups are produced in the presence of NaOH and can interact with the H$^+$ proton of the amine group on chitosan. Therefore, in the pH range below 6.5, the H$^+$ proton of chitosan is protected. These results obtained are almost in agreement with the other studies in the literature [48].

3.1.3. Degree of acetylation of chitosan

Infrared spectroscopy (IR) is a rapid technique for qualitatively evaluating DA by calculating the absorbance ratios of a characteristic band of an acetyl group on a band common to acetylated and deacetylated units [49]. The DDA is determined by the application of the law cited in the material and method part. The analysis of the infra-red spectra of the chitosan used makes it possible to deduce the degree of deacetylation DDA which is DDA = 59.27% and degree of acetylation DA = 40.73% using Eqs. (1) and (2).

3.1.4. Chitosan analysis by SEM and EDS

The morphology of chitosan was taken using SEM. The SEM photograph of chitosan made from shrimp shells

Fig. 3. FTIR spectroscopy of chitosan (a) before adsorption, (b) after MB adsorption, and (c) after CR adsorption.
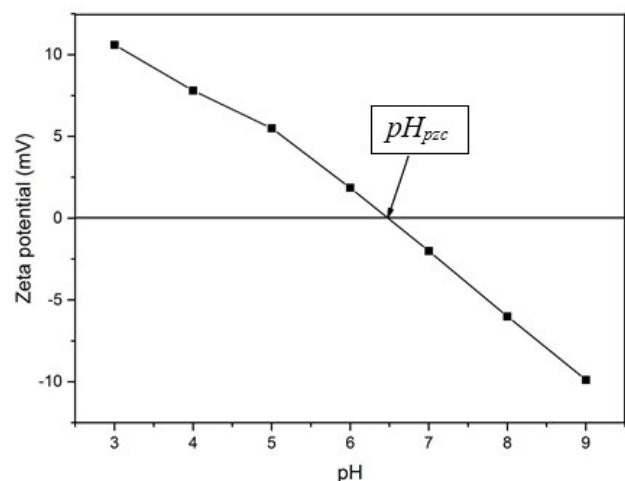
Fig. 4. Zeta potential measurements of chitosan.
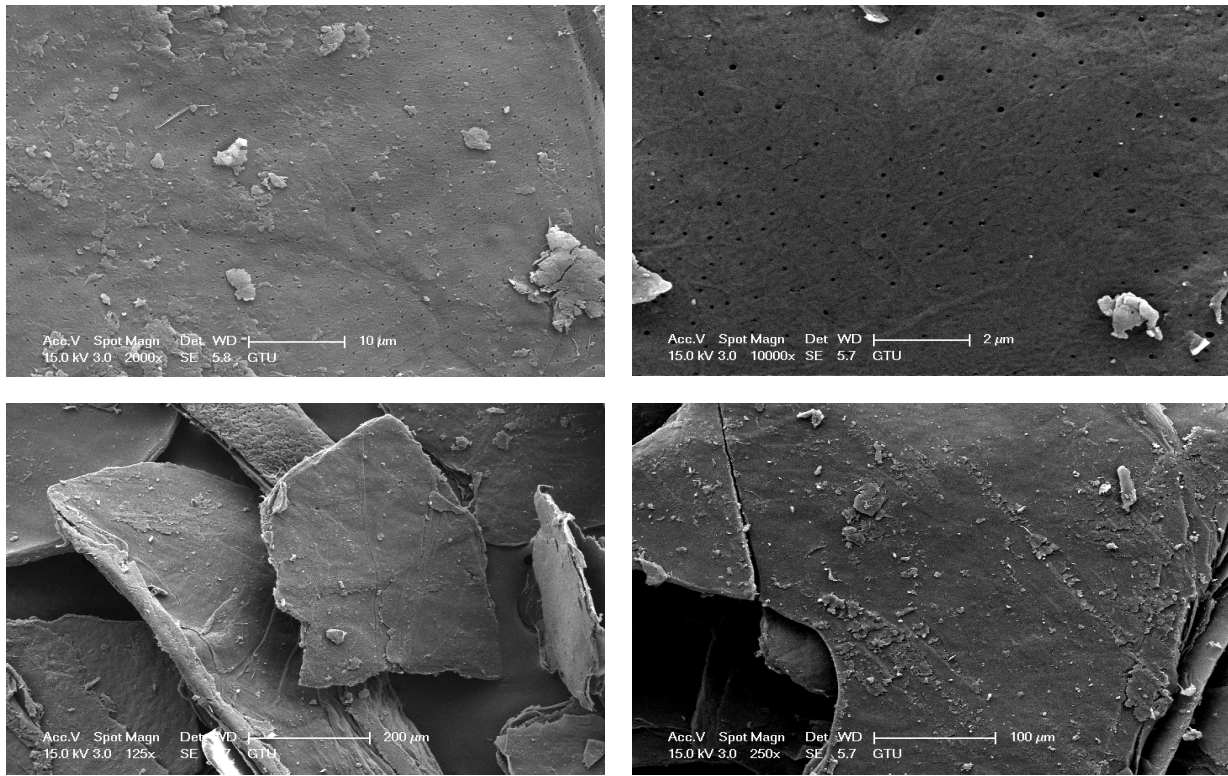
Fig. 5. SEM micrograph of prepared chitosan at different magnifications.
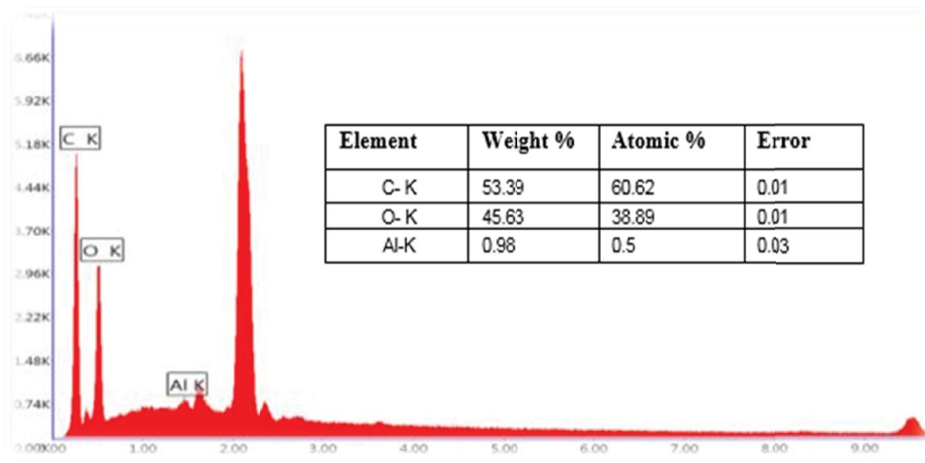
Fig. 6. EDS spectrum and surface elements found on chitosan.

of the Wilaya of Mostaganem, Algeria at various magnifications are shown in Fig. 5. It was observed that the extracted chitosan had flaked layers and that some areas were porous (magnification ×1,000). These results were agreeing with another study [50]. SEM with the add-on function of EDS is common spectroscopy to identify chemical elements distributed on the surface of the chitosan. EDS can also offer further supporting data on the substances contained on the surface. The composition of chitosan was determined by EDS Fig. 6 with different values of pH. The microanalysis of EDS was revealed 60% of carbon (C), 38% oxygen (O),

and 0.5% of aluminum (Al). Existence of aluminum with a small percentage back to metallization not showing up the nitrogen related to parameters of apparel.

3.2. Adsorption studies

3.2.1. Effect of contact time

It is necessary to determine an ideal contact time to reach equilibrium (i.e. the adsorbed quantity as well as the concentration remain unchangeable or stable). The equilibrium
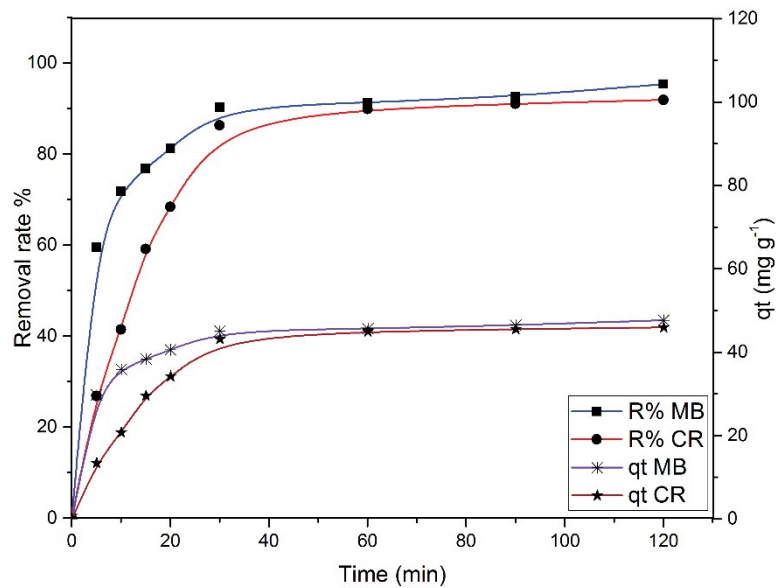
Fig. 7. Effect of the contact time on adsorption of MB and CR by the chitosan (m = 0.25g; C_0 = 100 mg L^{-1}; T = 20°C; V = 50 mL; pH 6.7 for MB and 7.1 for CR).
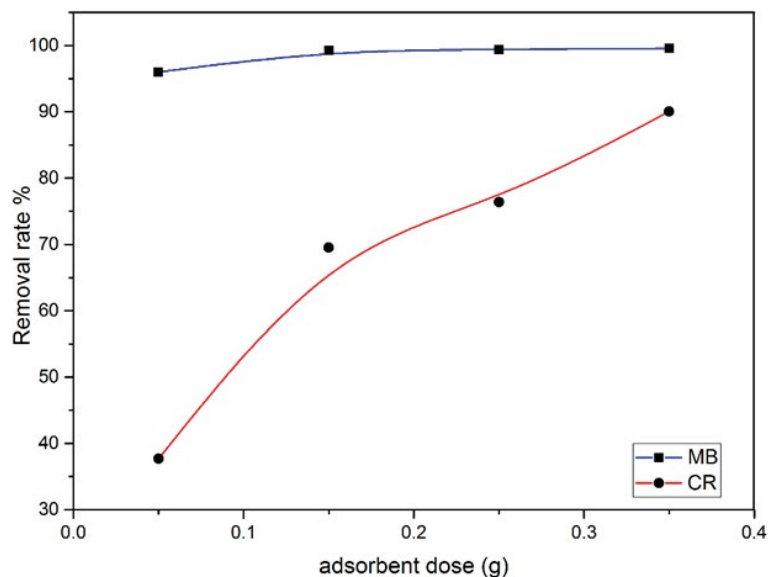
Fig. 8. Effect of the adsorbent mass on the adsorption of methylene blue and congo red (C_0 = 100 mg L^{-1}; t = 120 min; T = 20°C; V = 50 mL; pH 6.7 for MB and 7.1 for CR).

time is the moment where all the sites on the polysaccharide (chitosan) are filled and no possibility of fixation of MB and CR on the adsorbent material. As shown in Fig. 7, the adsorbed amount increases over time once the sites are all filled. During the first 30 min, it was found that maximum adsorption removal rates for both dyes were equal to over 90% with a removal amount of 43 mg g^{-1}.

3.2.2. Effect of adsorbent dose

The dose of the adsorbent can also affect the adsorption process efficiency. The effect of the amount of adsorbent

(chitosan) was examined using 0.05–0.35 g adsorbent masses and the outcomes are shown in Fig. 8. The results showed that the removal rate of MB rises very little with the mass of adsorbent, whereas the removal rate for CR increases with the increase in the amount of adsorbent. In other words, the elimination rate increases for CR from 38% to 90%, and the amount eliminated decreases from 38 to 13 mg g^{-1}. Because of the free sites on chitosan increase with the increased amount of adsorbent used. Once they exceed the desired number, the yield decreases automatically. This behavior can be described by the increase in the number of available adsorption surface places and the specific surface area of the

adsorbents resulting in a rise in the dye removal efficiencies the adsorbent dose increases. These results are consistent with the other works found in the literature [51,52].

3.2.3. Effect of the initial dye concentration

The effect of the initial dye concentrations on the removal of the MB and CR dyes (Fig. 9) was achieved by having various concentrations tested at room temperature. Both dye removal rates tend to decrease with increasing the initial concentrations. This is possibly due to the inadequate space of the adsorption sites on the adsorbent surface. However, a proportionate relationship is observed between the adsorbed quantity and a contradictory behavior between the dye elimination rate and initial concentration. These results can be explained by the theory of collision which asserts that the presence of more substances in a system increases the chance that molecules collide and accelerate the rate of reaction. Thus, increasing the dye concentration causes an increase in the number of dye ions in a solution involving better adsorption. It can also have said that the initial dye concentration increase leads to a rise in the mass grade between the solution and the adsorbent [53].

3.2.4. Effect of pH

pH of the solution is one of the other essential factors affecting the removal process. The pH range of 3–10 was chosen to study the pH effect on CR and MB dye adsorption on chitosan. HCl and NaOH solutions were used to adjust the pH of the solutions. MB is a cationic dye (positively charged) thus adsorptive removal is more favorable in acidic pH due to the phenomenon of electrostatic contact between the dye and chitosan. However, dye removal rates have not affected pH changes due to there are always more active sites available for both dye and the adsorbent at the experimental conditions studied. Fig. 10 further confirms this phenomenon and these results which are virtually similar. For CR dye, at

a pH of a solution more than pH_{pzc} a decrease in the CR elimination rate from 90% to 83% due to the deportation of chitosan [54] (the positively charged groups), in addition, there is also competition between the hydroxyl groups (OH⁻) of the solution and the CR anions for the positively charged adsorption sites (chitosan) [55]. For low pH (strongly acidic medium) the CR is slightly soluble [56] which decreases the elimination rate up to 79%, when the pH close to pH_{pzc} the CR is very soluble and the chitosan is always protonated [57], therefore a good rate of 90% elimination at pH = 6. The elimination of MB reduced at strongly acidic media (pH = 3) reflects the presence of excess H⁺ ions which compete with MB cations [58]. With a pH above 4, the elimination rate is between 92% and 93%.

3.3. Adsorption isotherm studies

The study of isotherms is fundamental for the description of the interactive behavior between the chitosan and the dye solution. The experimental equilibrium data were analyzed by two types of adsorption isotherms, Langmuir and Freundlich. The equilibrium adsorption curves of dye removal are depicted in Fig. 11 and as can be seen from this figure, the curve sharp of the isotherms rises suddenly initial stages due to the existence of readily accessible sites available. However, the curvature of plots was still raising at the end of the process conditions studied showed that there are still active sites available for dye adsorption.

The isotherm parameters and calculated R^2 correlation coefficients are given in Table 2. The result showed that both adsorption isotherm models were represented well by two isotherm model Langmuir (Fig. 12) and Freundlich (Fig. 13). The separation parameter values of R_L for dye adsorption processes were calculated using Eq. (8) and was found in the range of 0.03–0.538 indicating dye removal processes were favorable.

The linearized form of the Langmuir and Freundlich isotherms for the two dyes MB and CR are found to be linear with extremely high correlation coefficients $R^2 > 0.98$ as
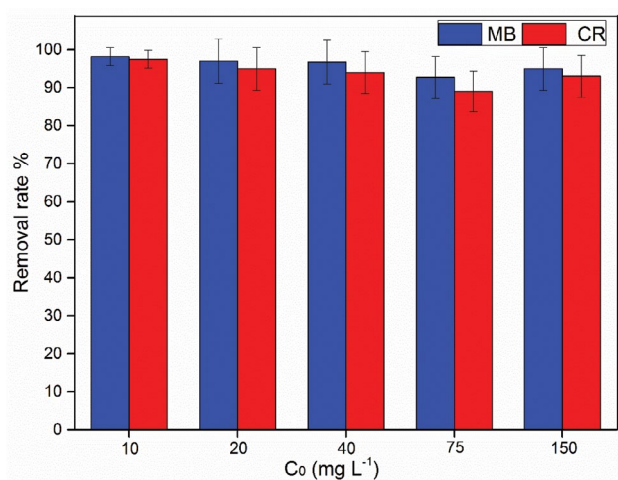
Fig. 9. Effect of the initial dye concentration on the adsorption of MB and CR on chitosan (pH = 4; m = 0.25 g; t = 120 min; T = 20°C; V = 50 mL).
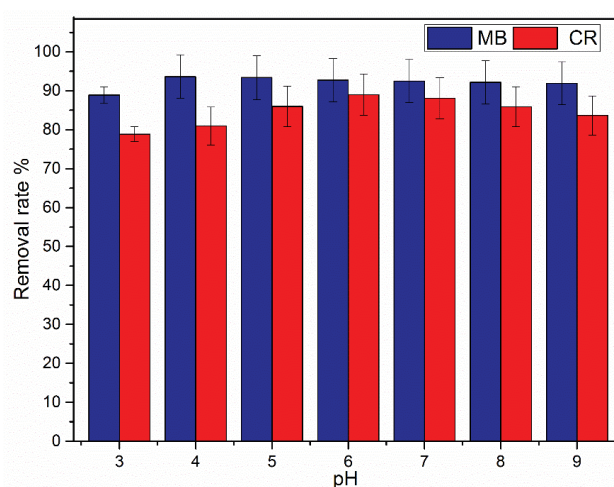
Fig. 10. pH effect on the adsorption of methylene blue and congo red by chitosan (C_0 = 100 mg L⁻¹; m = 0.25 g; t = 120 min; T = 20°C; V = 50 mL).
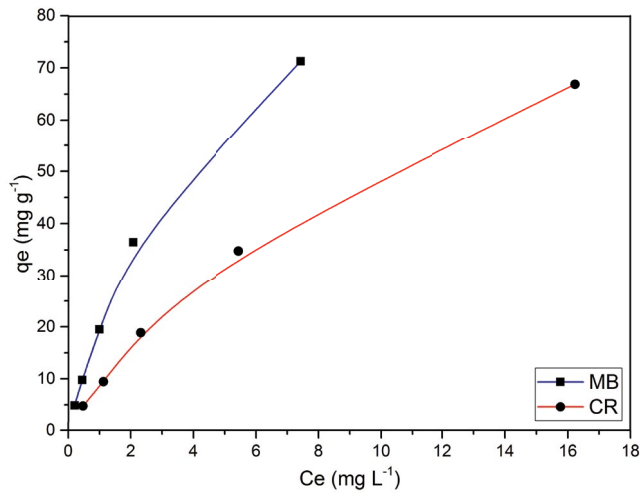
Fig. 11. Equilibrium plots for MB and CR adsorptions ($m = 0.25$ g; $T = 20°C$; $V = 50$ mL; pH 6.7 for MB and 7.1 for CR).
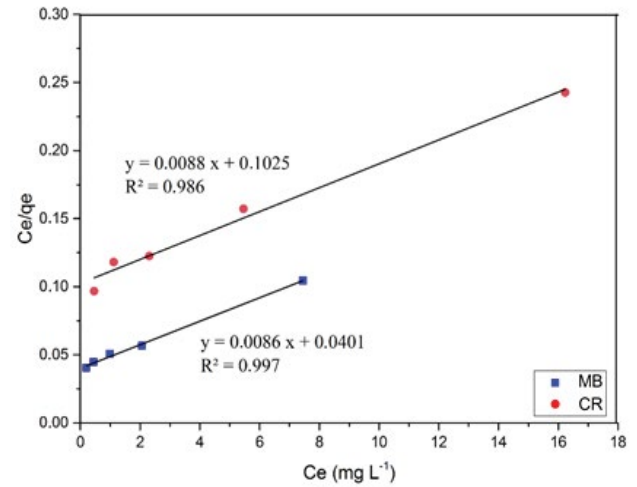
Fig. 12. Langmuir plot for adsorption of MB and CR ($m = 0.25$ g; $T = 20°C$; $V = 50$ mL).

Table 2
Isotherm constants and correlation coefficients of the isotherm models used

	Langmuir isotherm			Freundlich isotherm			Separation parameter
	Q_m (mg g^{-1})	b (L mg^{-1})	R^2	K_F (mg g^{-1})(L mg^{-1})$^{1/n}$	n	R^2	R_L
MB	116.3	0.2139	0.997	18.16	0.743	0.987	0.072–0.538
CR	113.6	0.0858	0.986	9.014	0.762	0.993	0.030–0.318
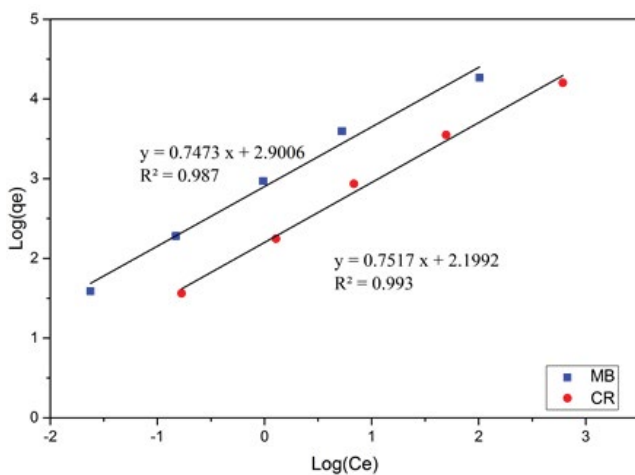
Fig. 13. Freundlich plot for the adsorption of MB and CR ($m = 0.25$ g; $T = 20°C$; $V = 50$ mL).
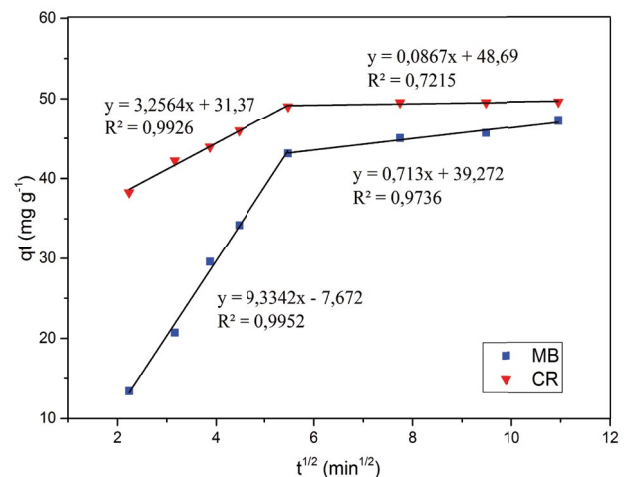
Fig. 14. Intra-particle diffusion model for the adsorption of MB and CR ($m = 0.25$ g; $C_0 = 100$ mg L^{-1}; $T = 20°C$; $V = 50$ mL).

shown in Table 2. Analysis of the modeling results showed that the MB adsorption issued of the Langmuir model had given the better fit of experimental data. Otherwise, the CR adsorption issued by the Freundlich model. The maximum adsorption capacity of MB and CR obtained from the Langmuir model is 116.3 and 113.6 mg g^{-1} respectively, indicates that chitosan has a good elimination efficiency for these two pollutants.

A brief comparative study of the adsorption capacity of the literature of various adsorbents for the elimination of MB and CR is presented in Table 3.

3.4. Kinetic of adsorption

The diffusion behavior of solid–liquid adsorption experiment was explored by the intra-particle diffusion

Table 3
Comparison of the maximum adsorption capacities (Q_m) of CR and MB on various adsorbents

Adsorbents	Pollutants	Q_m (mg g^{-1})	References
Chitosan nanocomposite beads	Methylene blue	36.25	[59]
Alginate-activated carbon composite	/	40.70	[4]
Crosslinked chitosan/bentonite composite	/	142.86	[58]
Biomass-based activated carbon by FeCl$_3$ activation	/	259.20	[60]
Chitosan	/	116.30	This work
Chitosan coated magnetic iron oxide	Congo red	56.66	[52]
Chitosan/montmorillonite nanocomposite	/	53.42	[53]
Carbon nanofiber@graphite	/	733.20	[61]
Chitosan	/	113.60	This work

Table 4
Calculated kinetic constants and correlation coefficients

	Pseudo-first-order			Pseudo-second-order			
	k_1 (min^{-1})	q_e (mg g^{-1})	R^2	$k_2 \times 10^4$ (g mg^{-1} min^{-1})	q_e (mg g^{-1})	h (mg g^{-1}min^{-1})	R^2
MB	0.096	32.063	0.875	3.960	50.251	1.000	0.997
CR	0.039	20.568	0.939	3.880	50.761	1.000	0.989

model. As shown in Fig. 14, separate two linear portions of intra-particle plots show that two different diffusion mechanisms take place throughout the elimination process. The first stage is the external mass transfer on the surface of adsorbent while the following linear part shows slow and final adsorption stages (Table 5). Therefore, it can safely be said that dye ions were firstly adsorbed by the external surface of the adsorbent, after reaching the saturation, dye ions passed in into pores within the chitosan and were adsorbed by the internal surfaces. Similar multi linearity has been reported in removal textile dye on permeable chitosan fibrous adsorptive material [62] and chitosan [64].

4. Conclusion

In this study, chitosan extracted and prepared from shoreline shells of the Mostaganem–Algerian littoral was used for the removal of two dyes MB and CR in an aqueous solution in batch mode. The adsorption capacity of both dyes by chitosan was made quickly with 30 min reaction time and over 90% removal percentage. The results are indicated that both isotherm models describe well the adsorption of MB and the CR on chitosan. From the results, it can be determined that chitosan can be used as an abundant and natural adsorbent material for the removal of dyes and also conclude that adsorption is a physicochemical process that remains simple is more feasible.

References

[1] G.M. Masters, P.E. Wendell, Introduction to Environmental Engineering and Science, Pearson New International Edition, Pearson Education Limited, Swiss, 2013.

Table 5
Constants and correlation coefficients of the intra-particle diffusion model

	k_{i1} (mg g^{-1} min$^{1/2}$)	R^2	k_{i2} (mg g^{-1} min$^{1/2}$)	R^2
MB	9.334	0.995	0.713	0.974
CR	3.256	0.992	0.087	0.721

[2] J. Liu, L. Zhang, Z. Liu, Environmental Pollution Control, Walter de Gruyter GmbH & Co KG, Germany, 2017.
[3] J. Sokolowska-Gajda, H.S. Freeman, A. Reife, Synthetic dyes based on environmental considerations. Part 2: iron complexes formazan dyes, Dyes Pigm., 30 (1996) 1–20.
[4] A. Boucherdoud, B. Bestani, N. Benderdouche, L. Duclaux, The use of calcium alginate-activated carbon composite material in fixed-bed columns for methylene blue removal from wastewater, Desal. Water Treat., 154 (2019) 356–368.
[5] K. Larbi, N. Benderdouche, L. Reinert, J.M. Leveque, S. Delpeux-Ouldriane, M. Benadjemia, B. Bestani, L. Duclaux, Tailored activated carbons prepared by phosphoric activation of apricot, date and loquat stones and their mixtures; relation between the pore size and the composition in biopolymer, Desal. Water Treat., 120 (2018) 217–227.
[6] R.M. Christie, Environmental Aspects of Textile Dyeing, Woodhead Publishing Limited, Elsevier, England, 2007.
[7] M.C. Collivignarelli, A. Abbà, M.C. Miino, S. Damiani, Treatments for color removal from wastewater: state of the art, J. Environ. Manage., 236 (2019) 727–745.
[8] M.A.M. Salleh, D.K. Mahmoud, W.A.W.A. Karim, A. Idris, Cationic and anionic dye adsorption by agricultural solid wastes: a comprehensive review, Desalination., 280 (2011) 1–13.
[9] K.G. Pavithra, K.P. Senthil, V. Jaikumar, R.P. Sundar, Removal of colorants from wastewater: a review on sources and treatment strategies, J. Ind. Eng. Chem., 75 (2019) 1–19.
[10] S. Karimifard, M.R. Alavi Moghaddam, Application of response surface methodology in physicochemical removal of dyes from wastewater: a critical review, Sci. Total Environ., 640–641 (2018) 772–797.

[11] E. Brillas, C.A. Martínez-Huitle, Decontamination of wastewaters containing synthetic organic dyes by electrochemical methods. An updated review, Appl. Catal., B, 166–167 (2015) 603–643.

[12] Y. Zhou, J. Lu, Y. Zhou, Y. Liu, Recent advances for dyes removal using novel adsorbents: a review, Environ. Pollut., 252 (2019) 352–365.

[13] K. Nadafi, M. Vosoughi, A. Asadi, M.O. Borna, M. Shirmardi, Reactive red 120 dye removal from aqueous solution by adsorption on nano-alumina, J. Water Chem. Technol., 36 (2014) 125–133.

[14] T.S. Kazeem, S.A. Lateef, S.A. Ganiyu, M. Qamaruddin, A. Tanimu, K.O. Sulaiman, S.M. Sajid Jillani, K. Alhooshani, Aluminium-modified activated carbon as efficient adsorbent for cleaning of cationic dye in wastewater, J. Cleaner Prod., 205 (2018) 303–312.

[15] M. Manconi, S. Mura, M.L. Manca, A.M. Fadda, M. Dolz, M.J. Hernandez, A. Casanovas, O. Díez-Sales, Chitosomes as drug delivery systems for C-phycocyanin: preparation and characterization, Int. J. Pharm., 392 (2010) 92–100.

[16] K.H. Chu, Removal of copper from aqueous solution by chitosan in prawn shell: adsorption equilibrium and kinetics, J. Hazard. Mater., 90 (2002) 77–95.

[17] J. Synowiecki, N.A. Al-Khateeb, Production, properties, and some new applications of chitin and its derivatives, Crit. Rev. Food Sci. Nutr., 43 (2003) 145–171.

[18] M. Rinaudo, Chitin and chitosan: properties and applications, Prog. Polym. Sci., 31 (2006) 603–632.

[19] J.R. Rangel-Mendez, R. Monroy-Zepeda, E. Leyva-Ramos, P.E. Diaz-Flores, K. Shirai, Chitosan selectivity for removing cadmium (II), copper (II), and lead (II) from aqueous phase: pH and organic matter effect, J. Hazard. Mater., 162 (2009) 503–511.

[20] F.S.C. dos Anjos, E.F.S. Vieira, A.R. Cestari, Interaction of indigo carmine dye with chitosan evaluated by adsorption and thermochemical data, J. Colloid Interface Sci., 253 (2002) 243–246.

[21] T.K. Saha, S. Karmaker, H. Ichikawa, Y. Fukumori, Mechanisms and kinetics of trisodium 2-hydroxy-1,1'-azonaphthalene-3,4', 6-trisulfonate adsorption onto chitosan, J. Colloid Interface Sci., 286 (2005) 433–439.

[22] A. Percot, C. Viton, A. Domard, Optimization of chitin extraction from shrimp shells, Biomacromolecules, 4 (2003) 12–18.

[23] F.A.A. Sagheer, M.A. Al-Sughayer, S. Muslim, M.Z. Elsabee, Extraction and characterization of chitin and chitosan from marine sources in Arabian Gulf, Carbohydr. Polym., 77 (2009) 410–419.

[24] R. Czechowska-Biskup, R.A. Wach, J.M. Rosiak, P. Ulański, procedure for determination of the molecular weight of chitosan by viscometry, Prog. Chem. Appl. *Chitin* Deriv., 17 (2018) 45–54.

[25] A. Domard, M. Rinaudo, Preparation and characterization of fully deacetylated chitosan, Int. J. Biol. Macromol., 5 (1986) 49–52.

[26] V. Mohanasrinivasan, M. Mishra, J.S. Paliwal, S.K. Singh, E. Selvarajan, V. Suganthi, C. Subathra Devi, Studies on heavy metal removal efficiency and antibacterial activity of chitosan prepared from shrimp shell waste, 3 Biotech., 4 (2013) 167–175.

[27] S. Lagergren, About the theory of so-called adsorption of soluble substances, Kungl Svenska Vetenskapsakad. Handl., 24 (1898) 1–39.

[28] H. Yuh-Shan, Citation review of Lagergren kinetic rate equation on adsorption reactions, Scientometrics, 59 (2004) 171–177.

[28] E. Bulut, M. Özacar, İ.A. Şengil, Equilibrium and kinetic data and process design for adsorption of congo red onto bentonite, J. Hazard. Mater., 154 (2008) 613–622.

[30] Y. Ho, G. McKay, Pseudo-second-order model for sorption processes, Process Biochem., 34 (1999) 451–465.

[31] W.J. Weber, J.C. Morris, Kinetics of adsorption on carbon from solution, J. Sanit. Eng. Div., 89 (1963) 31–60.

[32] I. Langmuir, The adsorption of gases on plane surfaces of glass, mica and platinum, J. Am. Chem. Soc., 40 (1918) 1361–1403.

[33] H. Freundlich, Oberflächeneinflüsse beim Bler und bei der Bierbereitung, Zeit Chem Ind Kol., 1 (1906) 152–152.

[34] F.-C. Wu, R.-L. Tseng, R.-S. Juang, Preparation of activated carbons from bamboo and their adsorption abilities for dyes and phenol, J. Environ. Sci. Health., Part A, 34 (1999) 1753–1775.

[35] B.V. Babu, S. Gupta, Adsorption of Cr(VI) using activated neem leaves: kinetic studies, Adsorption, 14 (2007) 85–92.

[36] K.R. Hall, L.C. Eagleton, A. Acrivos, T. Vermeulen, Pore- and solid-diffusion kinetics in fixed-bed adsorption under constant-pattern conditions, Ind. Eng. Chem. Fundam., 5 (1966) 212–223.

[37] M.B. Desta, Batch sorption experiments: Langmuir and Freundlich isotherm studies for the adsorption of textile metal ions onto teff straw (*Eragrostis tef*) agricultural waste, J. Thermodyn., 2013 (2013) 1–6.

[38] L.S. Campbell, B.E. Davies, Soil sorption of caesium modelled by the Langmuir and Freundlich isotherm equations, Appl. Geochem., 10 (1995) 715–723.

[39] A.O. Dada, Langmuir, Freundlich, Temkin and Dubinin–Radushkevich isotherms studies of equilibrium sorption of Zn^{2+} unto phosphoric acid modified rice husk, IOSR J. Appl. Chem., 3 (2012) 38–45.

[40] K.Y. Foo, B.H. Hameed, Insights into the modeling of adsorption isotherm systems, Chem. Eng. J., 156 (2010) 2–10.

[41] C.A. Coles, R.N. Yong, Use of equilibrium and initial metal concentrations in determining Freundlich isotherms for soils and sediments, Eng. Geol., 85 (2006) 19–25.

[42] L. Fan, C. Luo, M. Sun, X. Li, H. Qiu, Highly selective adsorption of lead ions by water-dispersible magnetic chitosan/graphene oxide composites, Colloids Surf., B, 103 (2013) 523–529.

[43] N. Sakkayawong, P. Thiravetyan, W. Nakbanpote, Adsorption mechanism of synthetic reactive dye wastewater by chitosan, J. Colloid Interface Sci., 286 (2005) 36–42.

[44] X.-Y. Huang, J.-P. Bin, H.-T. Bu, G.-B. Jiang, M.-H. Zeng, Removal of anionic dye eosin Y from aqueous solution using ethylenediamine modified chitosan, Carbohydr. Polym., 84 (2011) 1350–1356.

[45] A.H. Jawad, N.N.A. Malek, A.S. Abdulhameed, R. Razuan, Synthesis of magnetic chitosan-fly ash/Fe_3O_4 composite for adsorption of reactive orange 16 dye: optimization by Box–Behnken design, J. Polym. Environ., 8 (2020) 1068–1082.

[46] N.N.A. Malek, A.H. Jawad, A.S. Abdulhameed, K. Ismail, B.H. Hameed, New magnetic Schiff's base-chitosan-glyoxal/fly ash/Fe_3O_4 biocomposite for the removal of anionic azo dye: an optimized process, Int. J. Biol. Macromol., 146 (2020) 530–539

[47] M. Rinaudo, G. Pavlov, J. Desbrières, Influence of acetic acid concentration on the solubilization of chitosan, Polymer, 40 (1999) 7029–7032.

[48] L. Yan-Rung, C. Jung-Hao, T. Wei-Lun, C. Chia-Hung, L. Hao-Wu, A high efficiency UV-VIS organic photodetector by an inverted PTB7: PC71BM bulk heterojunction structure, IEEE Sensors, Busan, South Korea, 2015, pp. 1–3.

[49] J. Brugnerotto, J. Lizardi, F.M. Goycoolea, W. Argüelles-Monal, J. Desbrières, M. Rinaudo, An infrared investigation in relation with chitin and chitosan characterization, Polymer, 42 (2001) 3569–3580.

[50] A. Kucukgulmez, M. Celik, Y. Yanar, D. Sen, H. Polat, A.E. Kadak, Physicochemical characterization of chitosan extracted from *Metapenaeus stebbingi* shells, Food Chem., 126 (2001) 1144–1148.

[51] V.K. Singh, A.B. Soni, R.K. Singh, Comparative study of central composite and Box-Behnken design for the optimization of malachite green dye adsorption onto Sal seed activated char, J. Environ. Biol., 38 (2017) 849–858.

[52] H. Zhu, M. Zhang, Y. Liu, L. Zhang, R. Han, Study of congo red adsorption onto chitosan coated magnetic iron oxide in batch mode, Desal. Water Treat., 37 (2012) 46–54.

[53] L. Wang, A. Wang, Adsorption characteristics of congo red onto the chitosan/montmorillonite nanocomposite, J. Hazard. Mater., 147 (2007) 979–985.

[54] D.H.K. Reddy, S.-M. Lee, Application of magnetic chitosan composites for the removal of toxic metal and dyes from aqueous solutions, Adv. Colloid Interface Sci., 201 (2013) 68–93.

[55] H.-Y. Zhu, R. Jiang, L. Xiao, Adsorption of an anionic azo dye by chitosan/kaolin/γ-Fe_2O_3 composites, Appl. Clay Sci., 48 (2010) 522–526.

[56] Y. Bulut, H. Karaer, Adsorption of methylene blue from aqueous solution by crosslinked chitosan/bentonite composite, J. Dispersion Sci. Technol., 36 (2014) 61–67.

[57] G. Rojas, J. Silva, J.A. Flores, A. Rodriguez, M. Ly, H. Maldonado, Adsorption of chromium onto cross-linked chitosan, Sep. Purif. Technol., 44 (2005) 31–36.

[58] G. Crini, Kinetic and equilibrium studies on the removal of cationic dyes from aqueous solution by adsorption onto a cyclodextrin polymer, Dyes Pigm., 77 (2008) 415–426.

[59] I. Rahmi, M. Irfan, Methylene blue removal from water using H_2SO_4 crosslinked magnetic chitosan nanocomposite beads, Microchem. J., 144 (2019) 397–402.

[60] S.K. Theydan, M.J. Ahmed, Adsorption of methylene blue onto biomass-based activated carbon by $FeCl_3$ activation: equilibrium, kinetics, and thermodynamic studies, J. Anal. Appl. Pyrolysis, 97 (2012) 116–122.

[61] Y. Shen, L. Li, K. Xiao, J. Xi, Constructing three-dimensional hierarchical architectures by integrating carbon nanofibers into graphite felts for water purification, ACS Sustainable Chem. Eng., 4 (2016) 2351−2358.

[62] I.M. Lipatova, L.I. Makarova, A.A. Yusova, Adsorption removal of anionic dyes from aqueous solutions by chitosan nanoparticles deposited on the fibrous carrier, Chemosphere, 212 (2008) 1155–1162.

[63] Y. Chen, W. Long, H. Xu, Efficient removal of acid red 18 from aqueous solution by in-situ polymerization of polypyrrole-chitosan composites, J. Mol. Liq., 287 (2019) 110888.

[64] R.D.C. Soltani, A.R. Khataee, M. Safari, S.W. Joo, Preparation of bio-silica/chitosan nanocomposite for adsorption of a textile dye in aqueous solutions, Int. Biodeterior. Biodegrad., 85 (2013) 383–391.